AD-A047 174 PENNSYLVANIA STATE UNIV UNIVERSITY PARK APPLIED RESE--ETC F/G 20/4
COLLAPSE OF TURBULENT WAKES IN STABLY STRATIFIED MEDIA.(U)
AUG 77 S HASSID N00017-73-C-1418
UNCLASSIFIED TM-77-237 NL

1 OF 1
ADA047 174

END
DATE FILMED
1 - 78
DDC

(12) B.S.

COLLAPSE OF TURBULENT WAKES IN STABLY STRATIFIED MEDIA

S. Hassid

Technical Memorandum
File No. TM 77-237
10 August 1977
Contract No. N00017-73-C-1418

Copy No. 5

The Pennsylvania State University
APPLIED RESEARCH LABORATORY
Post Office Box 30
State College, PA 16801

Approved for Public Release
Distribution Unlimited

NAVY DEPARTMENT

NAVAL SEA SYSTEMS COMMAND

UNCLASSIFIED

SECURITY CLASSIFICATION OF THIS PAGE (When Date Entered)

REPORT DOCUMENTATION PAGE

READ INSTRUCTIONS BEFORE COMPLETING FORM

1. REPORT NUMBER: TM-77-237	2. GOVT ACCESSION NO.
3. RECIPIENT'S CATALOG NUMBER	
4. TITLE (and Subtitle): COLLAPSE OF TURBULENT WAKES IN STABLY STRATIFIED MEDIA.	5. TYPE OF REPORT & PERIOD COVERED: Technical Memorandum
6. PERFORMING ORG. REPORT NUMBER	
7. AUTHOR(s): S. Hassid	8. CONTRACT OR GRANT NUMBER(s): N00017-73-C-1418
9. PERFORMING ORGANIZATION NAME AND ADDRESS: Applied Research Laboratory, Post Office Box 30, State College, PA 16801	10. PROGRAM ELEMENT, PROJECT, TASK AREA & WORK UNIT NUMBERS
11. CONTROLLING OFFICE NAME AND ADDRESS: Naval Sea Systems Command, Washington, DC 20352	12. REPORT DATE: 10 August 1977
	13. NUMBER OF PAGES: 29
14. MONITORING AGENCY NAME & ADDRESS (if different from Controlling Office): 31p.	15. SECURITY CLASS. (of this report): UNCLASSIFIED
	15a. DECLASSIFICATION/DOWNGRADING SCHEDULE

16. DISTRIBUTION STATEMENT (of this Report)

Approved for public release. Distribution unlimited.
Per NAVSEA - Nov. 9, 1977.

17. DISTRIBUTION STATEMENT (of the abstract entered in Block 20, if different from Report)

18. SUPPLEMENTARY NOTES

19. KEY WORDS (Continue on reverse side if necessary and identify by block number)

turbulence
wakes
collapse
energy
stratified media
decay

20. ABSTRACT (Continue on reverse side if necessary and identify by block number)

A simple turbulent energy model and a calculation procedure are proposed, which are able to reproduce the main features of the collapse of turbulent wakes behind towed or self propelled bodies in stratified environments. The predictions of the model are shown to be in good agreement with the detailed experimental data of Lin & Pao, as well as with the flow visualization experiments of other workers.

DD FORM 1 JAN 73 1473 EDITION OF 1 NOV 65 IS OBSOLETE

391 007

UNCLASSIFIED

SECURITY CLASSIFICATION OF THIS PAGE (When Date Entered)

Subject: Collapse of Turbulent Wakes in Stably Stratified Media

References: See page 22.

Abstract: A simple turbulent energy model and a calculation procedure are proposed, which are able to reproduce the main features of the collapse of turbulent wakes behind towed or self propelled bodies in stratified environments. The predictions of the model are shown to be in good agreement with the detailed experimental data of Lin & Pao, as well as with the flow visualization experiments of other workers.

Acknowledgment: This work was sponsored by the Naval Sea Systems Command, Code NSEA-03133.

Nomenclature

$A, A', A'', c_1, c_2, c_{1T},$ $c_{2T}, c_T, c_{\varepsilon 1}, c_{\varepsilon 2}, \sigma_\varepsilon$	constants in the model
c_D	drag coefficient
D	body diameter
Fr	Froude number ($=U_o/D\ N$)
g	acceleration due to gravity
g_i	acceleration due to gravity vector
H	wake height
k	turbulent energy per unit volume
N	Brunt - Väisälä frequency
P	mean pressure
P_s	pressure deviation from hydrostatic state
R	Richardson number ($R^{1/2} = r_o\sqrt{\beta\ \alpha g/V_o}$
Ri	Richardson number ($= H^2N^2/k$)
r_o	initial radius of mixed region
T	mean temperature
t_{col}	time to start of collapse
U^i	mean velocity vector
U_d	velocity defect
U_D	velocity defect at the centerline
U_o	body velocity
U, V, W	streamwise, horizontal cross-stream and vertical cross-stream mean velocity components
u^i	fluctuating velocity vector
u, v, w	streamwise, horizontal cross-stream and vertical cross-stream fluctuating velocity component

$\overline{u},\overline{v},\overline{w}$	root mean square fluctuating velocity components
W	wake width
x^i	position vector
x,y,z	streamwise, horizontal cross-stream and vertical cross-stream coordinates, respectively
Z	wake half-width
$z_{1/2}$	distance between centerline and point where k = k(0)/4

Greek Symbols

α	temperature gradient of undisturbed fluid
β	volumetric expansion coefficient
ε	turbulent energy dissipation rate per unit volume
θ	temperature fluctuation
ν_v,ν_w	eddy diffusivity coefficients for momentum in the horizontal and vertical direction, respectively
ν_{Tv},ν_{Tw}	eddy diffusivity coefficients for heat in the horizontal and vertical directions, respectively
ρ	density
ρ_o	density at the centerline

List of Figures

INTRODUCTION

A turbulent wake in a stably stratified fluid exhibits some peculiar features which are not encountered in wakes in nonstratified media. Whereas axisymmetric wakes in homogeneous fluids increase indefinitely in width under the action of the diffusive turbulent forces, wakes in stably stratified environments are known to reach a maximum vertical extent and subsequently collapse to a minimum height. At the same time, under the combined action of turbulent diffusion and gravitational forces, they increase in the horizontal direction faster than they would in a neutral medium. Furthermore, since the decrease in the vertical extent is associated with a reduction in potential energy, gravitational internal waves are generated, which propagate through the surrounding fluid. (See Fig. 1.)

The first experimental investigation of this phenomenon was conducted by Schooley & Stewart [1], who used a flow visualization technique to observe the wake behind a self-propelled body. The same flow has since been documented in detail by Stockhausen, Clark & Kennedy [2], Lin & Pao [3], [4] and Stromm [5], whereas Pao & Lin [6], [7] focused on the wake behind a towed body in a stably stratified medium. Van der Watering, Tulin & Wu [8], Sumdaram et al. [9] and Meritt [10] investigated the collapse of mixed turbulent regions, generated by different means in quiescent, stably stratified media. These phenomena are closely related to the decay of momentumless wakes in such media, since turbulence in a momentumless wake is known to behave in a way similar to turbulence behind a point source. Wu [11] has observed the collapse of a tube of homogeneous, non-turbulent fluid in a stably stratified environment and the resulting wave pattern.

Theoretical investigations by Wessel [12] and Young & Hirt [13] focus on the collapse of a nonturbulent mixed region; this flow, however, differs from the collapse of the turbulent mixed region: whereas the latter reaches a final finite width, the former collapses indefinitely, until the fluid in the mixed region reaches the equilibrium level. The only theoretical treatment of the mixed region is by Vasiliev et al. [14]. The turbulence model used by these authors, however, does not predict any collapse, but only a slowing down of the rate of growth of the turbulent region. Furthermore, they neglect the nonlinear terms of the Navier Stokes equations. It is not clear that this approximation is justified because these are the very terms that cause the collapse. Finally, they make no comparison with experimental data and give no predictions for the streamwise velocity component in wake flows.

In this work it is proposed to use a simple turbulent flow model, coupled with a computational procedure, which will enable one to describe and document the phenomenon of collapse of turbulent wakes in stratified media.

THE FUNDAMENTAL EQUATIONS

Consider the wake behind a body moving with uniform velocity in a stably stratified medium with uniform temperature (or density) gradient. (The application of the model to salinity-stratified media is straightforward). Assuming the Boussinesq approximation to be valid (i.e., that the specific weight of the fluid is variable but its density can be considered constant) one obtains the following form for the Reynolds stress and continuity equations

$$U_j \frac{\partial U_i}{\partial x_j} + \frac{1}{\rho} \frac{\partial P}{\partial x_i} = \beta g_i T - \frac{\partial}{\partial x_j} \overline{u_i u_j} \qquad (1)$$

$$\frac{\partial U_i}{\partial x_i} = 0 \quad . \qquad (2)$$

In addition, the following simplifying assumptions will be made:

(a) The flow is elliptic in z and y and parabolic in x,

(b) $$U_o >> U_d \quad , \qquad (3)$$

where U_o is the velocity of the body and U_d is the local velocity defect, and

(c) $$| \overline{vw} | << \overline{w^2} \quad . \qquad (4)$$

Thus the equations take the following form:

$$U_o \frac{\partial U_d}{\partial x} + V \frac{\partial U_d}{\partial y} + W \frac{\partial U_d}{\partial z} + \frac{\partial \overline{u^2}}{\partial x} = - \frac{1}{\rho} \frac{\partial P_s}{\partial x} - \frac{\partial \overline{uv}}{\partial y} - \frac{\partial \overline{uw}}{\partial z} \quad , \qquad (5)$$

$$U_o \frac{\partial V}{\partial x} + V \frac{\partial V}{\partial y} + W \frac{\partial V}{\partial z} + \frac{\partial \overline{v^2}}{\partial y} = - \frac{1}{\rho} \frac{\partial P_s}{\partial y} \quad , \qquad (6)$$

$$U_o \frac{\partial W}{\partial x} + V \frac{\partial W}{\partial y} + W \frac{\partial W}{\partial z} + \frac{\partial \overline{w^2}}{\partial z} = - \frac{1}{\rho} \frac{\partial P_s}{\partial z} - \beta g(T - \alpha z) \quad , \qquad (7)$$

and

$$\frac{\partial V}{\partial y} + \frac{\partial W}{\partial z} = 0 \quad . \qquad (8)$$

Here P_s is the deviation of the pressure from the unperturbed hydrostatic pressure, whereas αz is the unperturbed temperature distribution, which is assumed linear.

By differentiating Eq. (6) with respect to y and Eq. (7) with respect to z and adding, a Poisson equation for the pressure can be obtained:

$$\frac{\partial^2}{\partial y^2}\left(\frac{P_s}{\rho} + \overline{v^2}\right) + \frac{\partial^2}{\partial z^2}\left(\frac{P_s}{\rho} + \overline{w^2}\right) = -\beta g \frac{\partial}{\partial z}(T - \alpha z) \quad . \tag{9}$$

In addition, the following equation governs the transport of temperature:

$$U_o \frac{\partial T}{\partial x} + V \frac{\partial T}{\partial y} + W \frac{\partial T}{\partial z} = -\frac{\partial}{\partial y}\overline{v\theta} - \frac{\partial}{\partial z}\overline{w\theta} \quad . \tag{10}$$

In order to solve the above system of equations, closure approximations are needed for the Reynolds stresses $\overline{uv}$ and $\overline{uw}$, as well as for the turbulent heat fluxes $\overline{v\theta}$ and $\overline{w\theta}$. These will be discussed in the following section.

THE TURBULENT FLOW MODEL

Recently, the Reynolds stress model has become increasingly popular in computational investigations of turbulent flow. For flows in wakes behind both towed and self-propelled bodies, however, the simpler k-ε model gives results which are in better agreement with experiment. (See Hassid [15]). Needless to say, of course, the k-ε model is also preferable because of its lower requirements in computer storage and time.

The closure used here is essentially based on the model of McGuirk and Rodi [16]. Transport equations are used for both the turbulent energy k and the dissipation rate ε and gradient diffusion forms for the Reynolds stresses. However, the expressions for the latter quantities are derived from invariant second order models by neglecting the advection and turbulent transport terms.

The expressions for $\overline{u_i u_j}$ and $\overline{u_i \theta}$ are

$$\frac{\overline{u_i u_j}}{k} = \frac{(1-c_2)}{c_1}\frac{\Pi_{ij}}{\varepsilon} - \frac{2}{3}\frac{(1-c_1-c_2)}{c_1}\delta_{ij} \tag{11}$$

where

$$\Pi_{ij} = -\left(\overline{u_i u_k}\frac{\partial U_j}{\partial x_k} + \overline{u_j u_k}\frac{\partial U_i}{\partial x_k}\right) - \left(g_i\overline{u_j\theta} + g_j\overline{u_i\theta}\right) \tag{12}$$

$$\overline{u_i\theta} = -\frac{k}{c_{1T}\varepsilon}\left[\overline{u_i u_k}\frac{\partial T}{\partial x_k} + (1-c_{2T})\left(\overline{u_k\theta}\frac{\partial U_i}{\partial x_k} + \beta\, g_i\overline{\theta^2}\right)\right] \quad . \tag{13}$$

$\overline{\theta^2}$, too, is calculated assuming equilibrium between production and dissipataion of this quantity. It is also assumed that the rate of destruction of the temperature variance $\overline{\theta^2}$ is proportional to the mechanical dissipation

$$\overline{\theta^2} = -\frac{2}{c_T}\frac{k}{\varepsilon}\overline{u_j\theta}\frac{\partial T}{\partial x_j} \quad . \tag{14}$$

McGuirk and Rodi used their model to describe jet flows in stratified media. Wake flows differ from jet flows in that the latter are parabolic in y. Therefore, in our case, some further approximations are needed. As already stated, $\overline{vw}$ will be neglected in comparison to the normal Reynolds stress components. Thus, the equations for the turbulent heat fluxes are

$$-\overline{u\theta} = \frac{k}{c_{1T}\varepsilon}\left[\overline{uw}\frac{\partial T}{\partial z} + \overline{uv}\frac{\partial T}{\partial y} + (1-c_{2T})\left(\overline{w\theta}\frac{\partial U}{\partial z} + \overline{v\theta}\frac{\partial U}{\partial y}\right)\right] \tag{15}$$

$$-\overline{v\theta} = \frac{k}{c_{1T}\varepsilon}\overline{v\theta}\frac{\partial T}{\partial y} \tag{16}$$

$$-\overline{w\theta} = \frac{k}{c_{1T}\varepsilon}\left[\overline{w^2}\frac{\partial T}{\partial z} - (1-c_{2T})\,\beta\, g\,\overline{\theta^2}\right] \quad . \tag{17}$$

These equations will be further simplified by assuming that $\partial T/\partial y$ is much smaller than $\partial T/\partial z$. Although this assumption is not strictly true, the error caused will be small, both for weak stratification, because the dependence on $\partial T/\partial y$ is small in that case, and for strong stratification, because then $\partial T/\partial z$ is indeed much larger than $\partial T/\partial y$. Thus Eq. (14) becomes

$$\overline{\theta^2} = -\frac{2}{c_T}\frac{k}{\varepsilon}\overline{w\theta}\frac{\partial T}{\partial z} \quad . \tag{18}$$

Substituting Eq. (18) into Eq. (17) one finds

$$\overline{w\theta} = \frac{\frac{k\,\overline{w^2}}{c_{1T}\,\varepsilon}\frac{\partial T}{\partial z}}{1 + \frac{(1-c_{2T})}{c_T}\frac{k^2}{\varepsilon^2}\beta\, g\,\frac{\partial T}{\partial z}} \quad . \tag{19}$$

Now, from Eq. (11), one obtains the following expressions for $\overline{v^2}$ and $\overline{w^2}$

$$\overline{v^2} = -\frac{2}{3}\frac{(1-c_1-c_2)}{c_1}k \quad , \tag{20}$$

$$\overline{w^2} = -\frac{w}{3}\frac{(1-c_1-c_2)}{c_1}k - 2\,\beta\, g\,\frac{k}{\varepsilon}\overline{w\theta} \quad . \tag{21}$$

Substituting into Equations (16) and (19) one obtains

$$-\overline{v\theta} = \nu_{Tv}\frac{\partial T}{\partial y} = c\,\frac{k^2}{\varepsilon}\frac{\partial T}{\partial y} \quad , \tag{22}$$

$$-\overline{w\theta} = \nu_{Tw}\frac{\partial T}{\partial z} = \frac{c_\theta\,\frac{k^2}{\varepsilon}\frac{\partial T}{\partial z}}{1 + A\,\frac{k^2}{\varepsilon^2}\beta\, g\,\frac{\partial T}{\partial z}} \quad , \tag{23}$$

where

$$c_\theta = -\frac{2}{3}\frac{(1-c_1-c_2)}{c_1\, c_T} \quad , \tag{24}$$

and

$$A = \frac{2}{c_{1T}}\left[\frac{1-c_{2T}}{c_T} + \frac{1-c_2}{c_1}\right] \quad . \tag{25}$$

Turning to the equations for the Reynolds stress one has

$$\overline{uv} = -\frac{1-c_2}{c_1}\frac{k\, v^2}{\varepsilon}\frac{\partial U}{\partial y} \quad , \tag{26}$$

$$\overline{uw} = -\frac{(1-c_2)}{c_1}\left[\frac{k\,\overline{w^2}}{\varepsilon}\frac{\partial U}{\partial z} - 2\,\beta\, g\,\overline{u\theta}\right] \quad . \tag{27}$$

Again, using Equations (20) and (26) one obtains

$$-\overline{uv} = \nu_v \frac{\partial U}{\partial y} = c_M \frac{k^2}{\varepsilon}\frac{\partial U}{\partial y} \quad , \tag{28}$$

where

$$c_M = -\frac{2}{3}\frac{(1-c_2)}{c_1}\frac{(1-c_1-c_2)}{c_1} \quad . \tag{29}$$

Neglecting, as already mentioned, $\partial T/\partial y$ in the equation for $\overline{u\theta}$ and substituting in Eq. (27), one ends with

$$-\overline{uw} = \nu_w \frac{\partial U}{\partial z} = c_M \frac{k^2}{\varepsilon}\frac{(1+A'F)}{(1+A''F)(1+AF)}\frac{\partial U}{\partial z} \quad , \tag{30}$$

where

$$F = \beta\, g\, \frac{k^2}{\varepsilon^2}\frac{\partial T}{\partial z} \quad , \tag{31}$$

and

$$A' = A - \left(2\,\frac{1-c_2}{c_1} + \frac{c_{2T}}{c_{1T}}\right)\frac{1}{c_{1T}} \quad , \tag{32a}$$

$$A'' = \frac{1-c_2}{c_{1T}\, c_1} \quad . \tag{32b}$$

As already mentioned, k and ε are calculated from the relevant transport equations:

$$U_o \frac{\partial k}{\partial x} + V \frac{\partial k}{\partial y} + W \frac{\partial k}{\partial z} = \frac{\partial}{\partial y}\left[\nu_v \frac{\partial k}{\partial y}\right] + \frac{\partial}{\partial z}\left[\nu_w \frac{\partial k}{\partial z}\right] + \nu_v \left(\frac{\partial U}{\partial y}\right)^2 + \nu_w \left(\frac{\partial U}{\partial z}\right)^2 + \beta\, g\, \overline{w\theta} - \varepsilon \quad , \tag{33}$$

$$U_o \frac{\partial \varepsilon}{\partial x} + V \frac{\partial \varepsilon}{\partial y} + W \frac{\partial \varepsilon}{\partial z} = \frac{\partial}{\partial y}\left[\frac{\nu_v}{\sigma_\varepsilon} \frac{\partial \varepsilon}{\partial y}\right] + \frac{\partial}{\partial z}\left[\frac{\nu_w}{\sigma_\varepsilon} \frac{\partial \varepsilon}{\partial z}\right] - c_{\varepsilon 2} \frac{\varepsilon^2}{k} + c_{\varepsilon 1} \frac{\varepsilon}{k}\left[\nu_v \left(\frac{\partial U}{\partial y}\right)^2 + \nu_w \left(\frac{\partial U}{\partial z}\right)^2 + \beta\, g\, \overline{w\theta}\right] . \tag{34}$$

Here the model differs from the one of McGuirk and Rodi because these authors claim that gravitational production does not appear in the equation for ε. It was found that such an assumption leads to unrealistically low values for k. It should be mentioned that there is wide disagreement among different research groups on the question of the influence of buoyant forces on the ε equation.

The constants used are

c_1	c_2	$c_{\varepsilon 1}$	$c_{\varepsilon 2}$	σ_ε	c_{1T}	c_{2T}	c_T
2.2	.55	1.44	1.92	1.3	3.2	.5	1.25

Of all the approximations used the neglect of $\partial T/\partial y$, which was necessary in order to obtain the gradient forms for the Reynolds stress equations, is the one likely to cause the greatest error. Notice however,

that for the non-buoyant case, the expressions derived above are exact.

METHOD OF SOLUTION

The system of equations to be solved consists of the x and y momentum equations

$$U_o \frac{\partial U_d}{\partial x} + V \frac{\partial U_d}{\partial y} + W \frac{\partial U_d}{\partial z} + \frac{\partial}{\partial x}\left(\frac{P_s}{\rho} + \overline{v^2}\right) + \frac{\partial}{\partial x}\left(\overline{u^2} - \overline{v^2}\right) =$$

$$\frac{\partial}{\partial y}\left[\nu_v \frac{\partial U_d}{\partial y}\right] + \frac{\partial}{\partial z}\left[\nu_w \frac{\partial U_d}{\partial z}\right] \qquad (35)$$

$$U_o \frac{\partial V}{\partial x} + V \frac{\partial V}{\partial y} + W \frac{\partial V}{\partial z} + \frac{\partial}{\partial y}\left(\frac{P_s}{\rho} + \overline{v^2}\right) = 0 \quad , \qquad (36)$$

the transport equation for temperature

$$U_o \frac{\partial T}{\partial x} + V \frac{\partial T}{\partial y} + W \frac{\partial T}{\partial z} = \frac{\partial}{\partial y}\left(\nu_{Tv} \frac{\partial T}{\partial y}\right) + \frac{\partial}{\partial z}\left(\nu_{Tw} \frac{\partial T}{\partial z}\right) \quad , \qquad (37)$$

the Poisson equation for pressure

$$\frac{\partial^2}{\partial y^2}\left(\frac{P_s}{\rho} + \overline{v^2}\right) + \frac{\partial^2}{\partial z^2}\left(\frac{P_s}{\rho} + \overline{w^2}\right) + \frac{\partial^2}{\partial z^2}\left(\overline{w^2} - \overline{v^2}\right) = \beta\, g\, \frac{\partial}{\partial z}\left(T - \alpha z\right) \quad , \qquad (38)$$

the continuity equation (Eq. 8), the transport equations for the turbulent energy k (Eq. 33), and the dissipation rate ε (Eq. 34). In addition, the following expressions for $\overline{u^2}-\overline{v^2}$ and $\overline{w^2}-\overline{v^2}$ can be derived from Eq. (11)

$$\overline{u^2} - \overline{v^2} = -\frac{(1-c_2)}{c_1}\left(\overline{uv}\frac{\partial U}{\partial y} + \overline{uw}\frac{\partial U}{\partial z}\right) \qquad (39)$$

and

$$\overline{w^2} - \overline{v^2} = \frac{(1-c_2)}{c_1}\,\beta\, g\, \overline{w\theta} \quad . \qquad (40)$$

This system was converted into a set of difference equations. Forward differencing was used in the x direction, centered differencing for the diffusive terms and upwind differencing for the lateral transport terms.

The mesh system used (Fig. 2) consists of an inner mesh AEFG in which the turbulent processes occur and an outer mesh, in which there is no turbulence. The outer mesh was three times as large as the inner mesh. The reason is that both experimental evidence and computer calculations suggest that the waves caused by the collapse of a nonturbulent mixed region advance twice the original width of that region after two Brunt-Väisälä periods. Since there are very few experimental data for times larger than two Brunt-Väisälä periods and in addition, the wave phenomena are much weaker when the mixed region is turbulent, this mesh was estimated to be adequate.

The mesh used was allowed to expand, so that the original growth due to turbulent diffusion can be simulated.

The following boundary conditions were used:

On AB,
$$V = \frac{\partial W}{\partial y} = \frac{\partial}{\partial y}\left(\frac{P_s}{\rho} + \overline{v^2}\right) = \frac{\partial U_d}{\partial y} = 0 \quad . \tag{41}$$

On AD,
$$\frac{\partial V}{\partial z} = W = \frac{\partial}{\partial z}\left(\frac{P_s}{\rho} + \overline{w^2}\right) = \frac{\partial U_d}{\partial z} = 0 \quad . \tag{42}$$

On BC,
$$V = \frac{\partial W}{\partial z} = P_s = U_d = 0 \quad . \tag{43}$$

On CD,
$$\frac{\partial V}{\partial y} = W = P_s = U_d = 0 \quad . \tag{44}$$

For k and ε, the boundary conditions were

On EF and FB, $$k = \varepsilon = 0 \quad . \tag{45}$$

On AE, $$\frac{\partial k}{\partial y} = \frac{\partial \varepsilon}{\partial y} = 0 \quad . \tag{46}$$

On AG, $$\frac{\partial k}{\partial z} = \frac{\partial \varepsilon}{\partial z} = 0 \quad . \tag{47}$$

Admittedly, some of these conditions are artificial and may result in errors as the wave fronts approach the mesh boundaries. It is estimated, however, that these errors will not be excessive for times less than two Brunt-Väisälä periods. As a check, the differential equations were solved using different boundary conditions and this did not significantly affect the results in the turbulent region.

RESULTS AND COMPARISON WITH EXPERIMENT

The main scaling parameter used by most investigators (Refs. 3, 6, 8, 9 and 10) for wake flows in stratified media is the Froude number, defined as

$$Fr = \frac{U_o}{N\,D} \tag{48}$$

where N is the Brunt-Väisälä frequency

$$N = \frac{1}{2\pi}\left(\frac{g}{\rho}\frac{\partial \rho}{\partial y}\right)^{1/2} \quad . \tag{49}$$

However, this scaling factor is not sufficient; what determines the extent that a momentumless wake will grow before collapsing is rather the Richardson number, which expresses the ratio between the potential energy and the turbulent kinetic energy at the origin

$$Ri = \frac{H^2N^2}{k} \quad . \tag{50}$$

The decay of momentumless wakes, even in the self-similar state, depends on such factors as the body shape (whether the body is blunt or slender), the propelling mechanism, etc. For non-buoyant flows behind slender bodies, the wake width is given by

$$\frac{H}{D} = .8\ (\frac{x}{D})^{.22} \quad . \tag{51}$$

(See Lin & Pao [3]). In Fig. 3a the influence of stratification on the wake behind such a body is shown. It is seen that the wake height and width become functions of Nx/U_o. Collapse starts when $Nx/U_o = 1/3$. The wake height decreases by 10% and then increases slightly. The wake width increases throughout the flow.

In the same figure, the correlations of Lin & Pao [3] are shown. The agreement between the predicted and the measured wake width is very good; however, our predictions overestimate the height of the wake. It must be noted, however, that Lin & Pao concede that there is considerable difficulty in estimating the wake width because of the irregular fluctuating nature of the outer wake boundary.

In Fig. 3b the width and the height of the wake behind a towed body in stratified flow are shown. Here the computed values of $2z_{1/2}$ are compared with the values of H and W measured by Pao & Lin [5] who claim that for drag wakes $H = 2z_{1/2}$. (In our computations, $H = 2.4z_{1/2}$.) It is seen that in wakes the first maximum is reached at a higher value of Nt than in momentumless wakes. Though the computations fail to reproduce the 10%

reduction in width recorded in the experiments, the agreement can be considered satisfactory, in view of the influence of stratification on the initial wake widths, which cannot be accounted for by the calculation procedure and in view of the experimental errors of flow visualization.

In Figs. 4a and 4b, the predicted wake width is compared with the results of Lin & Pao [4] for momentumless wakes and Pao & Lin [7] for drag wakes. The system of maxima and minima observed in these experiments is reproduced; there is however, a certain difference in phase probably due to the use of V=0 and W=0 as initial conditions.

In Fig. 5a and 5b it is seen that stratification results in slower decay of the velocity defect, both for drag wakes the momentumless wakes. Agreement with the experimental data is very good.

In Figs. 6a and 6b the decay of turbulent energy with and without stratification is shown. It is seen that in spite of the additional destruction of turbulent energy due to the stable stratification the difference in the turbulence levels is very small, especially in the momentumless wake. Agreement between theory and experiment is again very good in spite of the fact that the predicted $\sqrt{k}$ is compared with the measured $\overline{u}$.

Finally in Table I the predicted values of the maximum and the minimum heights as well as the collapse times of mixed regions and momentumless wakes are compared with their values as measured by several experimental workers.

In this table, t_{col} is the time (for mixed regions; distance divided by mean body velocity in momentumless wakes) at which the wake reaches the first maximum height, Z_{max} and Z_{min} are the maximum and minimum wake heights, respectively, whereas the Richardson number R is defined as

$$R^{1/2} = \frac{r_o \sqrt{\beta\, \alpha g}}{V_o} \quad . \qquad (52)$$

Table I

Collapse Time, Maximum Height and Minimum Height of Turbulent Mixed Regions in Stably Stratified Media

Reference		$t_{col}\sqrt{\beta\, \alpha g}$		Z_{max}/r_o		Z_{min}/r_o	
		Meas.	Pred.	Meas.	Pred.	Meas.	Pred.
Schooley & Stewart	Fr = 60	2.12	1.8	2.16	2.00	1.36	1.8
Stockhausen, Clark & Kennedy	Fr = 100	1.63	1.2	3.00	2.08	2.10	1.8
Van der Watering, Tulin & Wu	$R^{1/2}$ = 1.34	1.33	.92	1.51	1.26	1.11	.96
	1.56	1.48	.98	1.25	1.23	1.04	.91
	1.56	1.21	.98	1.31	1.26	1.06	.93
	2.19	1.35	.90	1.11	1.17	.90	.80
	2.19	1.35	.91	1.19	1.17	.90	.82
	3.09	1.40	.78	1.06	1.09	----	.68
	4.23	1.23	.51	.95	1.03	.77	.57
	4.27	1.05	.69	1.00	1.05	.83	.62
	1.56	1.12	.93	1.24	1.20	.94	.86
	1.57	1.12	.94	1.25	1.21	.89	.87
	2.28	.89	.74	1.20	1.13	1.00	.72
	3.21	1.25	.93	1.13	1.13	.94	.63
	2.06	1.05	.65	1.20	1.06	1.03	.63
	1.89	.73	.70	1.04	1.07	.88	.65
	3.69	1.07	.50	1.04	1.09	----	.58
	5.21	1.28	.58	.88	1.04	.77	.59
	5.29	1.18	.45	.95	1.02	.88	.55
Sundaram, Straton & Rehm	3.20	3.75	.72	1.54	1.12	1.07	.71
	2.80	2.40	.77	1.31	1.13	1.00	.74

where V_o is the initial rate of spreading and r_o is the initial radius of the mixed region. For the experiments of Schooley & Stewart and Stockhausen, Clark & Kennedy, r_o is the body diameter.

There are of course several sources of error in this table. Since no initial turbulent energy data were available, this quantity was deduced from the initial rate of spread and the equation

$$\frac{1}{\sqrt{k}} \frac{d Z}{d t} = .26 \qquad (53)$$

which is applicable to self-similar flow of momentumless wakes in nonstratified media. The initial turbulent energy and dissipation profiles were also assumed self-similar. Given, however, the very high Richardson numbers, it is very unlikely that the turbulent energy distribution may reach self similarity. Besides, the predicted value of t_{col} is the value of t when the wake height actually starts decreasing; typically, however, it has decreased by less than 5% at $t=2\ t_{col}$ and it is only then that it can be observed in a flow visualization experiment. Finally, for the experiments of Schooley & Stewart and Stockhausen, Clark & Kennedy, the production of turbulence by mean velocity gradients could not be taken into account.

In spite of all these considerations, it is thought that in view of the crudeness of the observation methods, the numerous assumptions needed for the calculation and the disagreement between the data themselves, even the order of magnitude agreement presented in Table I is satisfactory.

DISCUSSION AND CONCLUSIONS

The development of momentumless wakes, drag wakes and turbulent regions in stably stratified media was investigated using a simple turbulent energy - dissipation model. This is the simplest model that can be used for such flows; evidence from calculations in nonstratified media suggests

that for wake flows, this model is also more accurate than the more sophisticated Reynolds stress models.

The effect of stratification is expressed through a damping factor in the eddy diffusivity coefficients for vertical exchange of momentum and heat. The eddy diffusivities in the horizontal direction remain unaffected.

The stabilizing temperature gradient acts in two ways: (a) by reducing the turbulent fluctuation level in the vertical direction, thus impeding the ability of turbulence to diffuse in this direction; (b) by generating a mean flow pattern in which the vertical velocity is directed towards the horizontal symmetry plane and the horizontal velocity is directed away from the vertical symmetry plane. This flow pattern is due to the difference in weight between the fluid in the turbulent region and the surroundings. Thus, expansion of the mixed regions is impeded in the vertical direction and enhanced in the horizontal direction. The wake eventually reaches a maximum height in the vertical direction and shrinks. A system of maxima and minima in the height follows, which are separated by roughly one Brunt-Väisälä period.

The stratification is shown to slow the decay in the velocity defect, presumably as a result of the decrease in the rate of vertical exchange of momentum. It has very little effect on the total turbulent energy, because the destruction of turbulent energy by gravitational forces is balanced by the increase in the production (since the rate of decay of the mean velocity is smaller) and the decrease in the diffusion. These features of the flow, which are well documented in the experiments of Lin & Pao, are well reproduced by the model.

The model has, however, several limitations. It is not known whether it can account for the laminarization, that Lin & Pao claim occurs after four Brunt-Väisälä periods. The influence of gravitational negative production of turbulent energy on the dissipation equation is not certain and the particular assumption used in this model is only a tentative one, to be modified when a more realistic model is available. The calculation procedure used is not reliable for times larger than two Brunt-Väisälä periods, because at such times the artificially imposed boundary conditions may result in reflection of the waves generated by the collapse. In order to overcome this drawback, one may introduce a region of high viscosity on the outer part of the flow, so that outcoming waves are damped before they can be reflected. If this is done one may have a more reliable view of the wave pattern caused by the collapse but the computer requirements in storage and time would be significantly increased. Finally one should mention the artificial viscosity errors caused by the upwind differencing technique used to approximate the lateral transport terms which may partially account for the fact that the predicted collapse rate is lower (i.e., the final thickness is higher) than in many (but not all) experiments.

References

[1] Schooley, A. H. and Stewart, R. W., "Experiments with a Self-Propelled Body Submerged in a Fluid with Vertical Density Gradient," J. Fluid Mech., Vol. 15, Jan. 1963, pp. 83-96.

[2] Stockhausen, P. J., Clark, C. B. and Kennedy, J. F., "Three Dimensional Momentumless Wakes in Density Stratified Fluids," Dept. of Civil Eng., M.I.T., R. 93, June 1966.

[3] Lin, J. T. and Pao, Y. H., "Turbulent Wake of a Self-Propelled Slender Body in Stratified and Nonstratified Fluids: Analysis and Flow Visualization," Flow Research Inc., R. 11, July 1973.

[4] Lin, J. T. and Pao, Y. H., "Velocity and Density Measurements in the Turbulent Wake of a Propeller - Driven Slender Body in a Stratified Fluid," Flow Research Inc., R. 36, August 1974.

[5] Strom, G. H., "Wind Tunnel Experiments on Wakes in Stratified Flow Including Modeling Criteria and Development of Experimental Equipment," Polytechnic Inst. of New York, Dept. of Aerospace Eng. and Applied Mechanics, R. No. 76-11, June 1976.

[6] Pao, Y. H. and Lin, J. T., "Turbulent Wake of a Towed Slender Body in Stratified and Nonstratified Fluids: Analysis and Flow Visualizations," Flow Research Inc., R. No. 10, June 1973.

[7] Pao, Y. H. and Lin, J. T., "Velocity and Density Measurements in the Turbulent Wake of a Towed Slender Body in Stratified and Nonstratified Fluids," Flow Research Inc., R. 12, December 1973.

[8] Van der Watering, W. P. M., Tulin, M. P. and Wu, J., "Experiments on Turbulent Wakes in a Stable Density-Stratified Environment," Hydronautics, Inc., TR 231-24, Feb. 1969.

[9] Sundaram, T. R., Straton, J. E. and Rehm, R. C., "Turbulent Wakes in a Stratified Medium," Cornell Aeronautical Lab., R. AG-3018-A-1, November 1971.

[10] Meritt, C. E., "Wake Growth and Collapse in Stratified Flow," AIAA Journal, Vol. 12, July 1974, pp. 940-949.

[11] Wu, J., "Mixed Region Collapse with Internal Wave Generation in a Density Stratified Medium," J. Fluid Mech., Vol. 35, Feb. 1969, pp. 531-544.

[12] Wessel, W. R., "Numerical Study of the Collapse of a Perturbation in an Infinite Density Stratified Fluid," Physics of Fluids, Vol. 12, December 1969, pp. II171-176.

[13] Young, J. A and Hirt, C. W., "Numerical Calculation of Internal Wave Motions," J. Fluid Mechanics, Vol. 56, November 1972, pp. 265-276.

[14] Vasiliev, O. F., Kuznetsov, B. G., Lytkin, Y. M. and Chernykh, G. G., "Development of the Turbulent Mixed Region in a Stratified Medium," 9th ICHMT International Seminar on Turbulent Buoyant Convection, Dubrovnik, Yugoslavia, August 1976, pp. 123-136.

[15] Hassid S., "Similarity and Decay Laws in Momentumless Wakes," submitted to the Physics of Fluids, 1977. Also an Applied Research Labortory Technical Memorandum, File No. 77-187, May 1977.

[16] McGuirk, J. J. and Rodi, W., "Calculations of Three Dimensional Heated Surface Jets," 9th ICHMT International Conference on Turbulent Buoyant Convection, Dubrovnik, Yugoslavia, August 1976, pp. 275-287.

10 August 1977
SH:jep

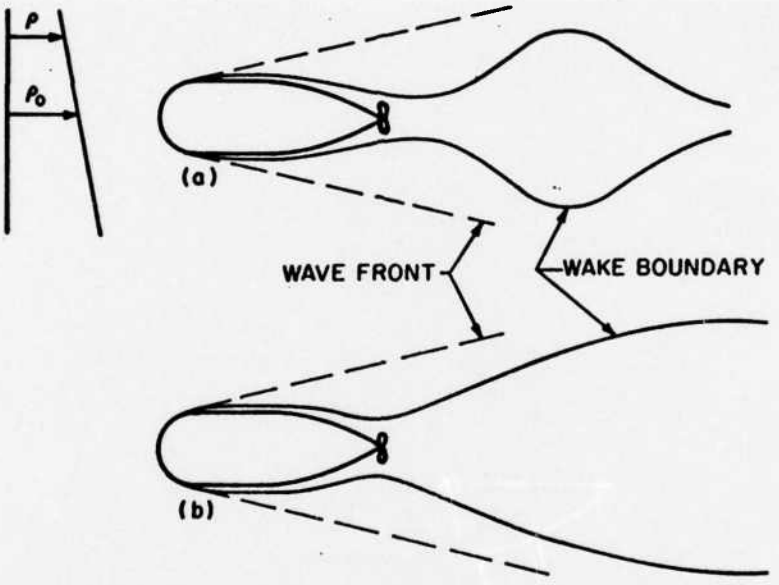

Figure 1 - Wake of a Self-Propelled Body in a Stably Stratified Fluid (a) Horizontal View, (b) Vertical View

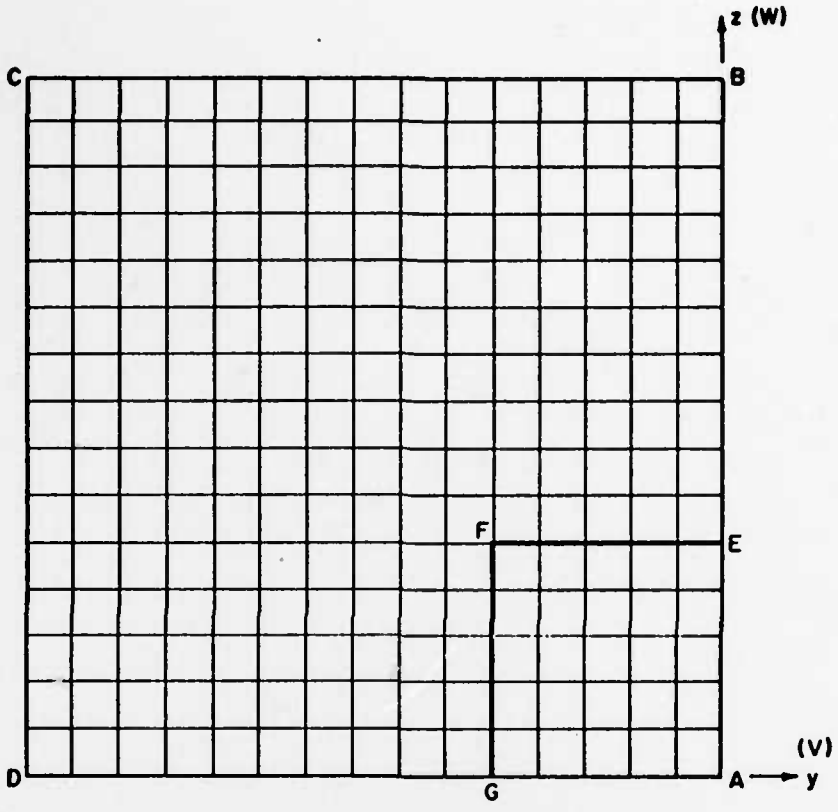

Figure 2 - Mesh System, First Quadrant

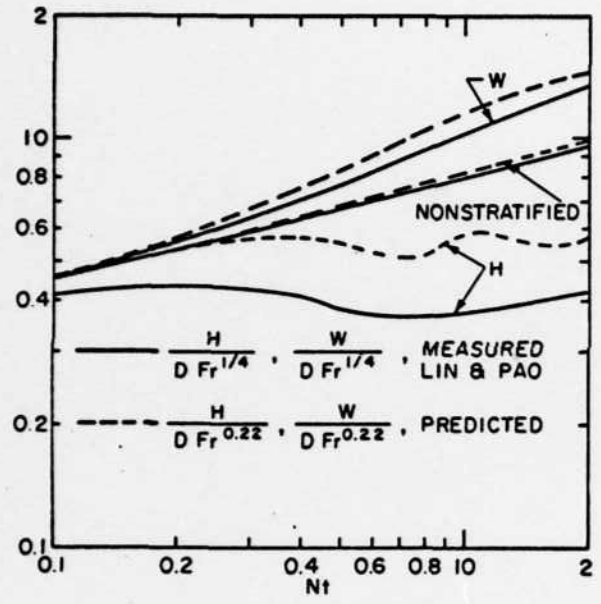

(a) Momentumless Wake, Data of Lin & Pao [3]

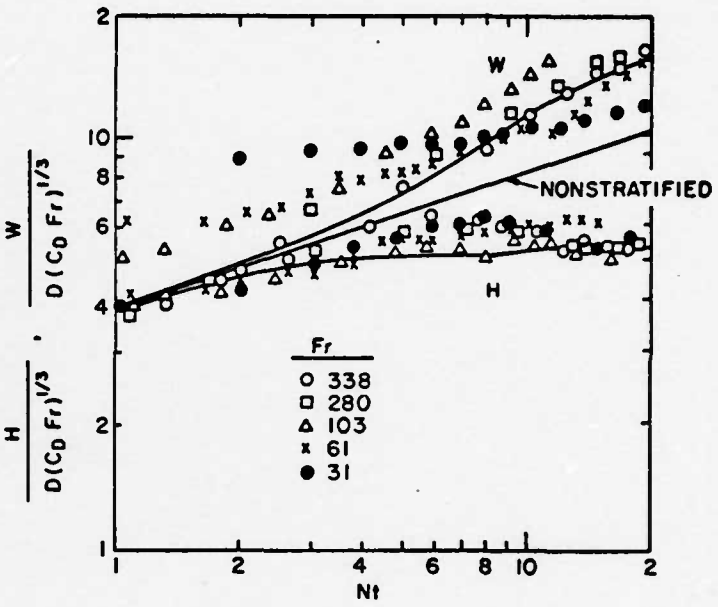

(b) Drag Wake, Data of Pao & Lin [6]

Figure 3 - Nondimensional Width and Height of a Wake in Stratified and Nonstratified Media

10 August 1977
SH:jep

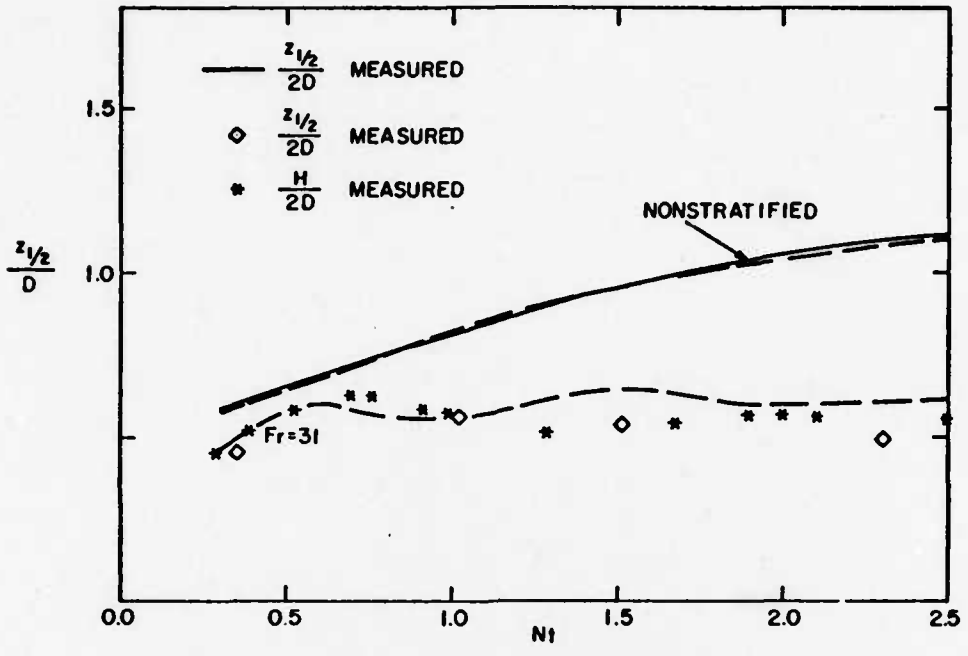

(a) Momentumless Wake, Data of Lin & Pao [4]

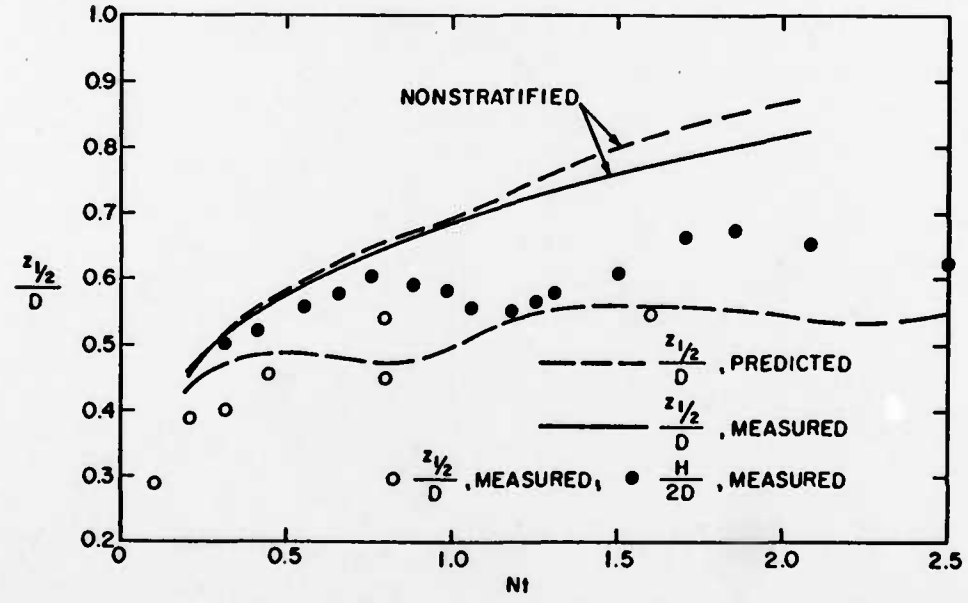

(b) Drag Wake, Data of Pao & Lin [7]

Figure 4 - Height of Wakes in Stratified and Nonstratified Media

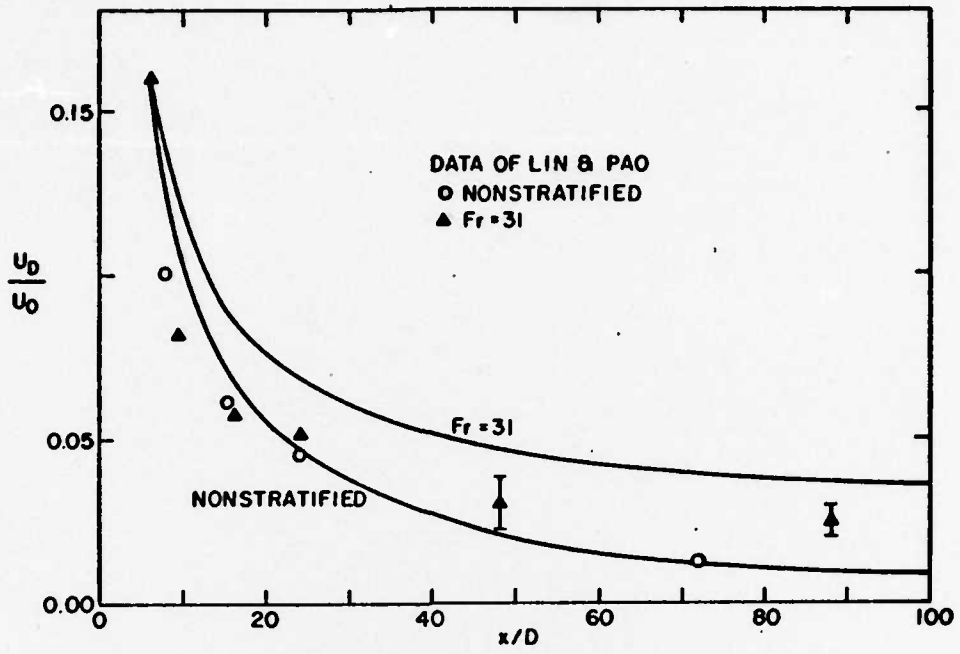

(a) Momentumless Wakes, Data of Lin & Pao

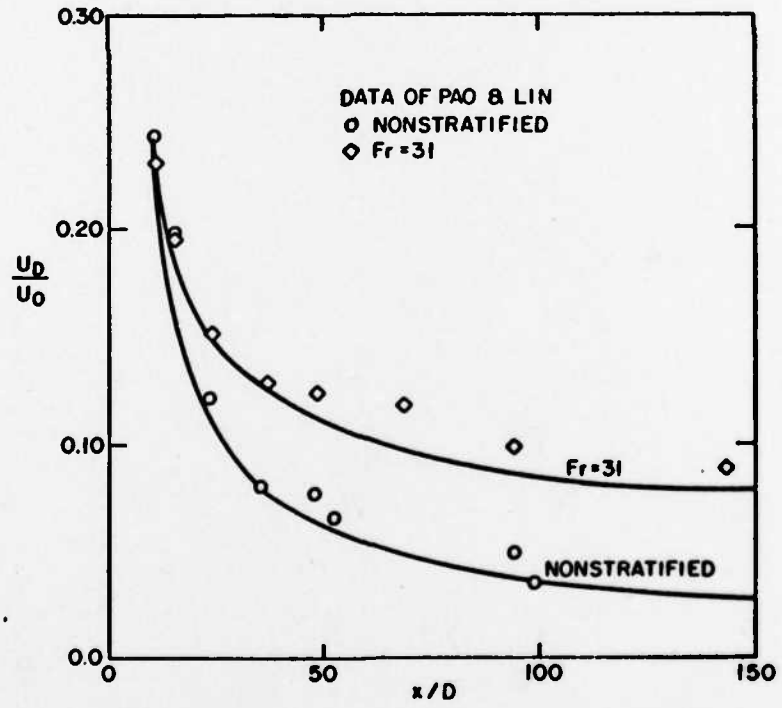

(b) Drag Wakes, Data of Pao & Lin [7]

Figure 5 - Centerline Velocity Defect in Wakes in Stratified and Nonstratified Media

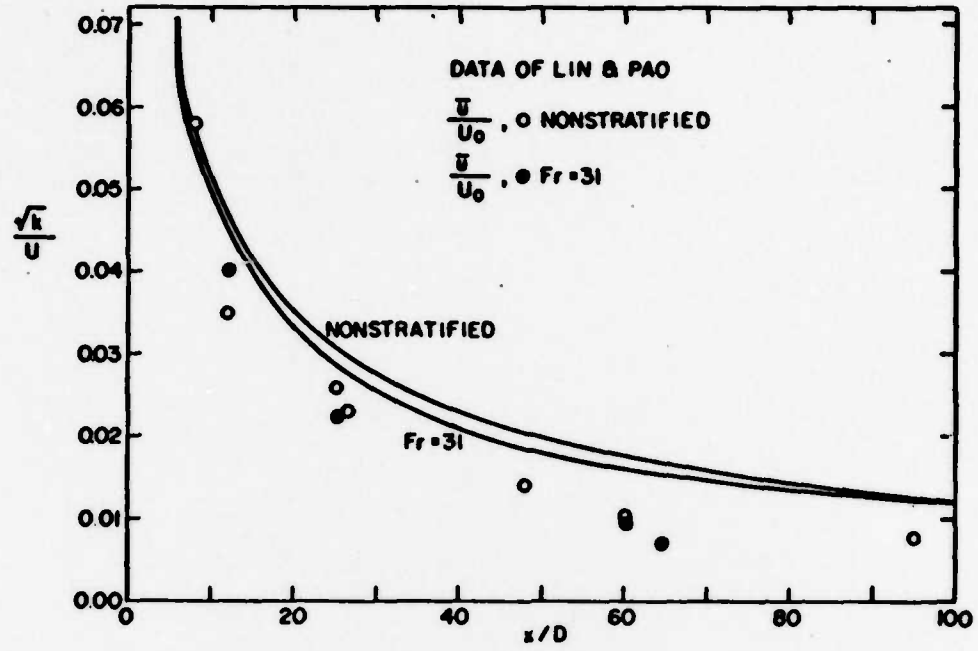

(a) Momentumless Wakes, Data of Lin & Pao [4]

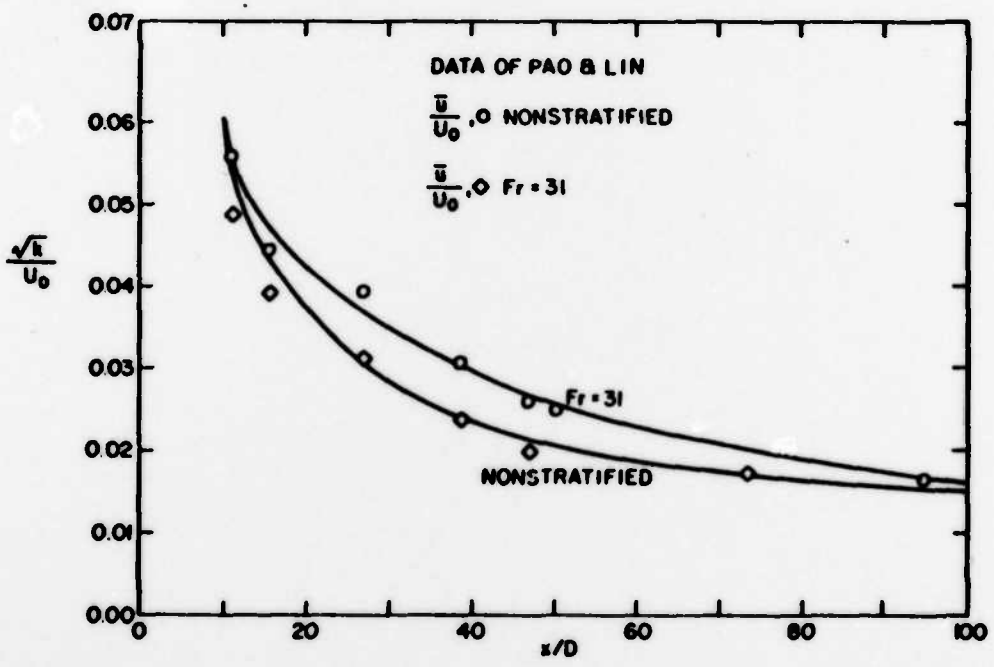

(b) Drag Wakes, Data of Pao & Lin [7]

Figure 6 - Centerline Turbulent Energy in Wakes in Stratified and Nonstratified Media

DISTRIBUTION LIST FOR UNCLASSIFIED TM 77-237 by S. Hassid, dated 10 August 1977

Commander
Naval Sea Systems Command
Department of the Navy
Washington, DC 20362
Attn: Library
Code NSEA-09G32
(Copy Nos. 1 and 2)

Naval Sea Systems Command
Attn: C. G. McGuigan
Code NSEA-03133
(Copy No. 3)

Defense Documentation Center
5010 Duke Street
Cameron Station
Alexandria, VA 22314
(Copy Nos. 4 - 15)

Defense Advanced Research Projects Agency
1400 Wilson Boulevard
Arlington, VA 22209
Attn: P. A. Selwyn, TTO
(Copy No. 16)

Naval Ocean Systems Center
San Diego, CA 92152
Attn: R. Buntzen
(Copy No. 17)

Headquarters
Naval Material Command
Washington, DC 20360
Attn: CDR K. Hastie
MAT-031
(Copy No. 18)

Commander
Naval Underwater Systems Center
Newport, RI 02840
Attn: G. Garosi
(Copy No. 19)

Flow Research, Inc.
1819 S. Central Avenue
Suite 72
Kent, WA 98031
Attn: J. Riley
(Copy No. 20)

JAYCOR, Inc.
1401 Camino Del Mar
Del Mar, CA 92014
Attn: Dr. J. H. Stuhmiller
(Copy No. 21)

Johns Hopkins University
Applied Physics Laboratory
Johns Hopkins Road
Laurel, MD 20910
Attn: L. Cronvich
(Copy No. 22)

Aerospace Corporation
P. O. Box 92957
Los Angeles, CA 90009
Attn: Dr. T. Taylor
(Copy No. 23)

Hydronautics, Inc.
Pindell School Road
Laurel, MD 20901
Attn: Dr. T. R. Sundaram
(Copy No. 24)

Office of Naval Research
800 N. Quincy Street
Arlington, VA 22217
Attn: R. Cooper
(Copy No. 25)

Office of Naval Research
Attn: S. Reed
(Copy No. 26)

Naval Research Laboratory
Washington, DC 20390
Attn: J. O. Elliot
Code 8300
(Copy No. 27)

Naval Research Laboratory
Attn: J. Witting
Code 8340
(Copy No. 28)

Naval Research Laboratory
Attn: J. Dugan
Code 8340
(Copy No. 29)

DISTRIBUTION LIST FOR UNCLASSIFIED TM 77-237 by S. Hassid, dated 10 August 1977 (continued)

Naval Research Laboratory
Attn: E. Rudd
Code 8310
(Copy No. 30)

TRW Systems
One Space Park
Redondo Beach, CA 90278
Attn: Dr. J. Chang
(Copy No. 31)

Physical Dynamics, Inc.
P. O. Box 1069
Berkeley, CA 94704
Attn: Dr. J. Thomson
(Copy No. 32)

Poseidon Research
11777 San Vicente Boulevard
Los Angeles, CA 90049
Attn: Dr. S. Crow
(Copy No. 33)

Science Applications, Inc.
P. O. Box 2351
La Jolla, CA 92037
Attn: Dr. K. Victoria
(Copy No. 34)

Dynamics Technology, Inc.
3838 Carson Street, Suite 110
Torrance, CA 90509
Attn: Dr. D. R. S. Ko
(Copy No. 35)

Arete Associates
2120 Wilshire Boulevard
Santa Monica, CA 90403
Attn: Dr. F. Fernandez
(Copy No. 36)

Science Applications, Inc.
8400 Westpark Drive
McLean, VA 22101
Attn: Dr. G. Roberts
(Copy No. 37)

SRI International
P. O. Box 1474
La Jolla, CA 92037
Attn: R. Leonard
(Copy No. 38)

Operations Research, Inc.
1400 Spring Street
Silver Spring, MD 20910
Attn: E. Holmboe
(Copy No. 39)

Operations Research, Inc.
Attn: R. Hoglund
(Copy No. 40)

Virginia Polytechnic Institute
and State University
P. O. Box 290
Blacksburg, VA 24061
Attn: Dr. J. Schetz
(Copy No. 41)

SRI International
1611 N. Kent Street
Arlington, VA 22209
Attn: Dr. D. LeVine
(Copy No. 42)

Institute for Defense Analyses
400 Army-Navy Drive
Arlington, VA 22202
Attn: J. C. Nolen
(Copy No. 43)

Institute for Defense Analyses
Attn: W. Wasylkiwskyj
(Copy No. 44)

Mr. S. Hassid
The Pennsylvania State University
Department of Aerospace Engineering
233 Hammond Building
University Park, PA 16802
(Copy No. 45)

DISTRIBUTION LIST FOR UNCLASSIFIED TM 77-237 by S. Hassid, dated 10 August 1977 (continued)

GTWT Library
The Pennsylvania State University
APPLIED RESEARCH LABORATORY
Post Office Box 30
State College, PA 16801
(Copy No. 46)


ATE
LMED